Applied Thermal Engineering 31 (2011) 1790–1797

Contents lists available at ScienceDirect

Applied Thermal Engineering

journal homepage: www.elsevier.com/locate/apthermeng

# Experimental characterization of heat transfer in non-boiling spray cooling with two nozzles

Yujia Tao [a], Xiulan Huai [a,*], Lei Wang [a], Zhixiong Guo [b]

[a] Institute of Engineering Thermophysics, Chinese Academy of Sciences, P.O. Box 2706, Beijing 100190, China
[b] Department of Mechanical and Aerospace Engineering, Rutgers, The State University of New Jersey, 98 Brett Road, Piscataway, NJ 08854, USA

ARTICLE INFO

*Article history:*
Received 7 September 2010
Accepted 16 February 2011
Available online 2 March 2011

*Keywords:*
Non-boiling
Spray cooling
Heat transfer characteristics

ABSTRACT

Heat transfer in a non-boiling spray cooling system with de-ionized water as the working fluid is experimentally investigated. An open-loop test system with two full-cone spray nozzles used to generate water droplets to a heated surface is established for the cooling of high-power devices. The effects of the liquid volume flow rate, the nozzle-to-surface distance and the liquid inlet temperature on the heat transfer are scrutinized. It is found that the non-boiling spray cooling system can remove high heat flux from a small surface while maintaining the surface at desirable low temperature. Increasing the liquid volume flow rate or reducing the liquid inlet temperature increases significantly the heat transfer coefficient. There exists an optimal nozzle-to-surface distance under which the heat transfer coefficient is maximized. It is also found that adding a surfactant to the working fluid with an appropriate concentration will further improve the heat transfer.



## 1. Introduction

Spray cooling can be employed to remove high heat flux from surfaces by impinging a large amount of liquid droplets generated by pressure atomizers on the surfaces. It has been shown that spray cooling yields a heat flux approximately an order of magnitude greater than pool boiling using the same liquid [1]. Traditionally, spray cooling is used to cool highly-heated surface, such as those in metallurgy, chemical and nuclear industry. The temperature of the heated surface could be up to 873–1273 K and film cooling heat transfer dominates [2]. Recently, spray cooling has received much attention in modern industrial and technological applications, such as the cooling of integrated electronic devices and high-power solid-state lasers while maintaining low surface temperature.

In a spray cooling process, lots of micro-droplets impact on a heated surface. A thin liquid film may be formed. If the surface temperature is lower than the saturation temperature of the spray liquid, boiling heat transfer is absent in the liquid film. This is called non-boiling spray cooling. The understanding of the heat transfer mechanism governing the heat removal process and the parametric studies in non-boiling spray cooling are quite limited due to the complicated random process in spray and the uncertainties in the interactions of various parameters. It is essential to make clear the heat transfer characteristics of the non-boiling spray cooling to enable systematic, practical system design.

The following observations from experimental studies have been reported in the literatures. Bonacina et al. [3] showed that the measured heat flux was proportional to the fraction of the solid surface wetted by the spray in the non-boiling regime. A heat transfer coefficient up to $1.5 \times 10^5$ W/m$^2$K and a heat flux up to $2.2 \times 10^6$ W/m$^2$ were obtained. Toda [4] obtained the critical heat flux to be about $3.0 \times 10^6$ W/m$^2$ in their experiments, which was greater than that of pool boiling. A linear $q - \Delta T$ relationship without subcooling was observed. It was suggested that the heat was conducted through the thin liquid film, followed by direct evaporation from the liquid-vapor surface. The thin-film heat transfer may be significantly contributed to the overall heat flux in the non-boiling spray cooling. Zheng et al. [5] studied the effects of nozzle inlet pressure, nozzle type, nozzle-to-surface distance and the mass flow rate on the heat transfer coefficient of non-boiling spray cooling. Fabbri et al. [6] conducted experiments on non-boiling spray cooling using HAGO nozzles to compare the performance of sprays and micro-jet arrays. Their experimental data showed that the heat transfer coefficient was independent of the wall to liquid temperature difference. And the spray performed better than the micro-jets at lower liquid flow rates; while the spray and the micro-jets had almost the same heat transfer rate at higher liquid flow rates.

The thickness of the liquid film on the surface was important for studying the heat transfer mechanism in non-boiling spray cooling.

* Corresponding author. Tel./fax: +86 10 8254 3108.
*E-mail address:* hxl@mail.etp.ac.cn (X. Huai).

1359-4311/$ – see front matter © 2011 Elsevier Ltd. All rights reserved.
doi:10.1016/j.applthermaleng.2011.02.025

**Nomenclature**

| | |
|---|---|
| $A$ | area of the heated surface ($m^2$) |
| $a$ | thermal diffusivity ($m^2/s$) |
| $C_D$ | flow coefficient |
| $D$ | equivalent diameter of the heated surface (m) |
| $d$ | mass median diameter of the droplets (m) |
| $d_{32}$ | Sauter mean diameter of the droplets (m) |
| $d_j$ | diameter of the nozzle exit (m) |
| $h$ | heat transfer coefficient ($W/(m^2\ K)$) |
| $h_1$ | distance between the test surface and the upper plane of the thermocouple (m) locations (m) |
| $h_2$ | distance between the two thermocouple location planes (m) |
| $h_3$ | nozzle-to-surface distance (m) |
| $k$ | thermal conductivity (W/(m K)) |
| $Nu$ | Nusselt number |
| $\Delta P$ | pressure difference between the nozzle exit and the heated surface (Pa) |
| $\Delta P_1$ | spray pressure drop between the liquid inlet and the atmosphere (Pa) |
| $Pr$ | Prandtl number |
| $Q$ | volume flow rate ($m^3/s$) |
| $q$ | heat flux ($W/m^2$) |
| $Re$ | Reynolds number |
| $T$ | temperature (K) |
| $T_{1,m}$ | arithmetic mean temperature at the upper plane (K) |
| $T_{2,m}$ | arithmetic mean temperature at the lower plane (K) |
| $u_0$ | mean velocity of the spray droplets impinged on the test surface (m/s) |
| $u_j$ | spray velocity at the nozzle exit (m/s) |
| $We$ | Weber number |

*Greek symbols*

| | |
|---|---|
| $\alpha$ | nozzle spray angle (rad) |
| $\nu$ | kinematic viscosity ($m^2/s$) |
| $\rho$ | liquid density ($kg/m^3$) |
| $\sigma$ | surface tension (N/m) |
| $\sigma_y$ | uncertainty of indirect measurement physical quantity |

*Subscripts*

| | |
|---|---|
| $l$ | liquid |
| $w$ | Surface |

Pautsch and Shedd [7] performed an experiment to measure the local mean thickness of liquid film using a non-intrusive optical technique, and found that the film thickness in the spray impact region did not change measurably with the applied heat flux within the measurement uncertainty. The result agreed with that found in their earlier study [8] in which the heat removal mechanism was dominated by single-phase behavior. An et al. [9] showed that the liquid film could be divided into a fluctuated layer and a laminar layer in non-boiling spray cooling. The smaller was the thickness; the better was the cooling effect. The thickness of the liquid film was in the magnitude from hundred-micron to kilo-micron under different test conditions.

A survey of the literature has shown that most of the researchers have concentrated on free non-boiling spray cooling in a large space or using a single nozzle. In some cases, cooling of the surfaces with high heat flux requires multiple nozzles. Little experimental data is currently available on the heat transfer with multiple nozzles. Ma et al. [10] and Amon et al. [11] presented that using multiple nozzles could effectively control the spray distribution on the heated surface and improve the cooling uniformity. Nguyen et al. [12] found that in the case of the same mass flow rate, increasing the number of nozzles could enhance the critical heat flux. Recently, Lin et al. [13] conducted an experiment to investigate the spray cooling curves using 48 nozzles to cool a heated copper block of $1.93 \times 10^{-3}$ $m^2$. The critical heat flux for this array was unfortunately found to be 34% lower than that on a heated surface of $2.0 \times 10^{-4}$ $m^2$ cooled by an 8-nozzle array. It is visible that the existing data are insufficient and many questions persist regarding the multiple nozzles heat transfer.

Considering the advantages of multiple nozzles and the limitation of space in practical heat removal for small devices, we established a non-boiling spray cooling system with a small heated surface of $2 \times 10^{-4}$ $m^2$ and two full-cone spray nozzles. The deionized water was used as the working fluid. The heat transfer characteristics of non-boiling spray cooling are presented. The effects of the liquid volume flow rate, the nozzle-to-surface distance, the liquid inlet temperature and the addition of surfactant on the heat transfer coefficient are examined.

## 2. Experimental apparatus

### 2.1. Test facility

The test facility consists of four parts: fluid delivery, spray, heater assembly and data acquisition. The open-loop fluid delivery system is comprised of two liquid tanks, a rotary vane pump, a preheater, a filter and the flow channels with control valves. A schematic of this test facility is shown in Fig. 1. Fluid leaving the liquid tank passes through the two nozzles and sprays onto the heated surface. A heat transfer process is completed when the liquid outflows from the spray chamber and returns to the reservoir. The preheater is used to regulate the liquid inlet temperature. The volume flow rate of each nozzle is adjusted by the bypass. The entire flow channels are made of plastic which can sustain the pressure up to $8 \times 10^5$ Pa.

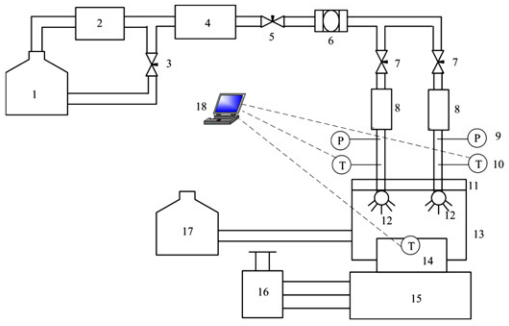


1-Liquid tank, 2-Rotary vane pump, 3-Bypass valve, 4-Preheater, 5-Control valve, 6-Filter, 7-Control valve, 8-Rotameters, 9- Pressure gages, 10-Thermocouples, 11-Two-nozzle plate, 12-Spray nozzles, 13-Spray chamber, 14-Thermocouples, 15-Block heater, 16-Booster, 17-Liquid reservoir, 18-Computer

**Fig. 1.** Schematic of the experimental setup.

### 2.2. Spray system

In the spray system, two commercially available full-cone spray nozzles with $d_j = 5.6 \times 10^{-4}\ m$ (TGSS0.4, Spraying Systems Co. Ltd) are housed in a stainless steel rectangle chamber. The nozzle-to-surface distance is adjustable in the range of $(7-22) \times 10^{-3}$ m. The maximum liquid volume flow rate of each nozzle is $8.67 \times 10^{-6}\ m^3/s$. The space dimensions of the spray chamber are 0.09 m high, 0.15 m long and 0.1 m wide. The frame of the four sides of the spray chamber is replaced with four pieces of high-temperature glasses to facilitate the observation of the spray conditions.

### 2.3. Heater assembly

A copper block heater consisted of six rod-type heaters is employed as the heat source in the experiments. The maximum power of each rod-type heater is 250 W. The actual input power of the block heater can be set by adjusting the input AC voltage of the booster. The structure of the heater is shown in Fig. 2(a). The upper surface of the heater with an area of $2 \times 10^{-4}\ m^2$ is used as the test surface. The heat flux on the test surface is assumed to distribute uniformly because the normal distance from the rod-type heater to the test surface is long enough. The block heater is housed in a stainless steel chamber with fiberfrax to minimize the heat transfer to the ambience. The block heater is inserted into the bottom plate of the spray chamber. Sealants are applied to prevent the liquid from leaking out from the gap between the chamber and the heater.

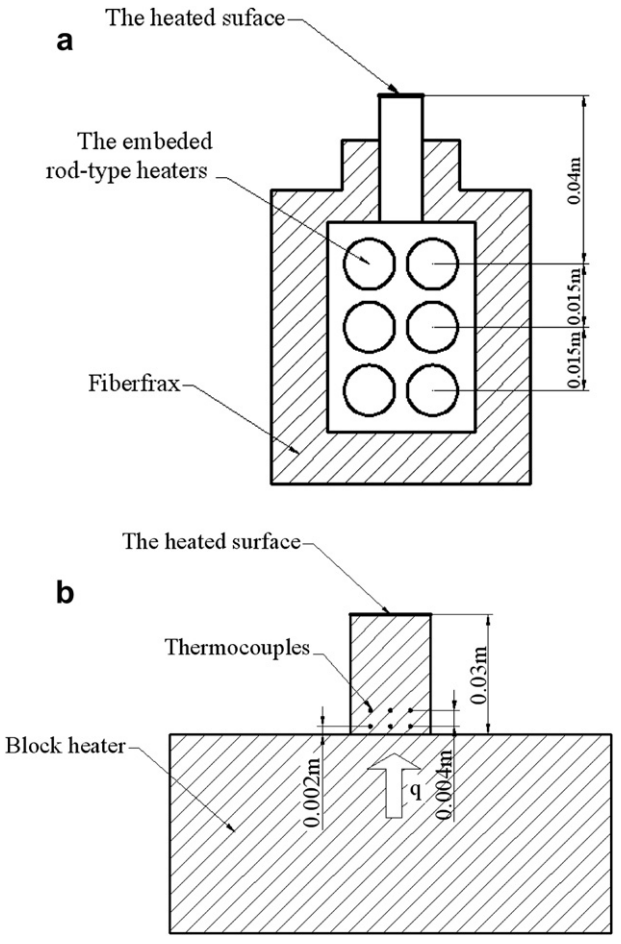


**Fig. 2.** (a) Structure of the block heater; (b) distribution of the thermocouples in the block heater.

### 2.4. Data acquisition system

The liquid volume flow rate, the liquid inlet pressure, the liquid inlet and outlet temperatures, the test surface temperature and the nozzle-to-surface distance are measured in the experiments. The test surface temperature is acquired by indirect measurement due to the thin liquid film on the surface and the continuous impact of droplets. Six K-type thermocouples with probe diameter of $5 \times 10^{-4}$ m are embedded into the holes drilled along the two planes in the block heater as shown in Fig. 2(b). The distance between the two thermocouple location planes is $4 \times 10^{-3}$ m. The distance between the test surface and the upper plane of the thermocouple locations is $2.4 \times 10^{-2}$ m. Such an indirect measurement will not ruin the flow and the convection boundary conditions near the surface. The heat flux on the test surface can be calculated by expression (1) on the basis of Fourier law of heat conduction:

$$q = k(T_{2,m} - T_{1,m})/h_2. \tag{1}$$

The average temperature of the test surface can be calculated by:

$$T_w = T_{1,m} - qh_1/k. \tag{2}$$

The thermocouple signals are send to a programmable scanner (7501, Yokogawa Co., Japan) and a display equipment (7503, Yokogawa Co., Japan) for showing and recording the temperature information. All the thermocouples are pre-calibrated.

### 2.5. Operating procedure

The operating steps are as follows:

(1) Prior to each test, we install the two-nozzle plate onto the spray chamber and adjust the liquid volume flow rate, the nozzle-to-surface distance and the liquid inlet temperature to the desirable values.
(2) The AC voltage is turned on when the spray becomes stable in order to avoid an over-high temperature at the test surface. The voltage is set at a low starting level.
(3) When the steady state heat transfer is achieved, the liquid volume flow rate, the liquid inlet pressure, the liquid inlet and outlet temperatures and the temperatures of the six thermocouples are measured respectively.
(4) Increase the AC voltage to each preset level and repeat step 3.
(5) Change the liquid volume flow rate, the liquid inlet temperature, the nozzle-to-surface distance and the working liquid, respectively; and repeat the above process.

The test conditions are shown in Table 1.

## 3. Measurement uncertainty and heat loss

The uncertainties of the liquid volume flow rate, the liquid inlet pressure, the temperature of the thermocouples and the distances are listed in Table 2. The uncertainties of the heat flux on the test surface, the flow coefficient and the test surface temperature can be calculated by:

$$\sigma_y = \sqrt{\sum_{i=1}^{m} (\partial f/\partial x_i)^2 \sigma_{x_i}^2}, \tag{3}$$

where $\partial f/\partial x_i$ is the error transfer coefficient.

From the computations, the uncertainties of the heat flux on the test surface, the test surface temperature and the flow coefficient

**Table 1**
Test conditions adopted.

| Influencing parameters | | | | | | | |
|---|---|---|---|---|---|---|---|
| Liquid volume flow rate for each nozzle ($\times 10^{-6}$ m$^3$/s) | 2.22 | 2.78 | 3.89 | 5.0 | 6.11 | 6.67 | |
| Nozzle-to-surface distance ($\times 10^{-2}$m) | 1.151 | | 1.451 | | 1.774 | | 2.109 |
| Liquid inlet temperature (K) | 278.6 | | 288.1 | | 300.6 | | |
| Working fluid | no surfactant | | with 100 ppm surfactant | | with 500 ppm surfactant | | |

are respectively ±6.5%, ±4.73% and ±9.4%. It is seen that the temperature uncertainty has the greatest contribution to the heat flux and the test surface temperature uncertainties. The liquid inlet pressure uncertainty has the greatest contribution to the flow coefficient uncertainty.

Fig. 3 shows the heat removal capability of the present experimental system. The *x*-axis is the input power and the *y*-axis is the ratio of the cooing power removed by the input power. Under the three different liquid volume flow rates ($2.78 \times 10^{-6}$, $3.89 \times 10^{-6}$ and $5.0 \times 10^{-6}$ m$^3$/s) for each nozzle, about 77.5% of the input power can be dissipated through the non-boiling spray cooling system. When the input power becomes larger, the heat removal capacity of the system reduces.

## 4. Results and discussion

### 4.1. Flow coefficients of the nozzles

Fig. 4 (a) and (b) show the pressure drop of the two nozzles under various liquid volume flow rates and the flow coefficient curves of the two nozzles, respectively. Because the spray chamber is open to the ambience, the spray pressure drop is the pressure difference between the liquid inlet and the atmosphere. It is seen from Fig. 4(a) that the spray pressure drop increases with the increase of the liquid volume flow rate. The slope of the two curves varies with the magnitude of the volume flow rate. In the lower volume flow rate, e.g., $Q < 3.89 \times 10^{-6}$ m$^3$/s, the slope of the curves is relatively small. When the volume flow rate exceeds $3.89 \times 10^{-6}$ m$^3$/s, the slope of the curves will increase. The results agree with the variations of the flow coefficients of the two nozzles as shown in Fig. 4(b).

The flow coefficients of the nozzles can be calculated by:

$$C_D = 4Q/\left(\pi d_j^2\sqrt{2\Delta P_1/\rho}\right) \tag{4}$$

It is seen from Fig. 4(b) that the flow coefficients reduce with the increase of the spray pressure drop, particularly when the pressure drop is lower than $2.0 \times 10^5$ Pa. When the pressure drop exceeds $2.0 \times 10^5$ Pa, the decrease of the flow coefficients slows down. The resistance losses of the flow channels will increase when the pressure drop becomes large, which results in the decrease of the flow coefficient. Since the variations of the pressure drop with the volume flow rate for the two nozzles are similar, it indicates that the pressure and flow distribution of the system is uniform.

**Table 2**
The uncertainties of the direct measurement quantities.

| The direct measurement physical quantities | Uncertainties |
|---|---|
| Liquid volume flow rate | ±5.5% |
| Liquid inlet pressure | ±1.2% |
| Temperature of the thermocouples in the block heater | ±1.7% |
| Distance between the test surface and the upper plane of the thermocouple locations | ±0.5% |
| Distance between the two thermocouple location planes | ±0.083% |

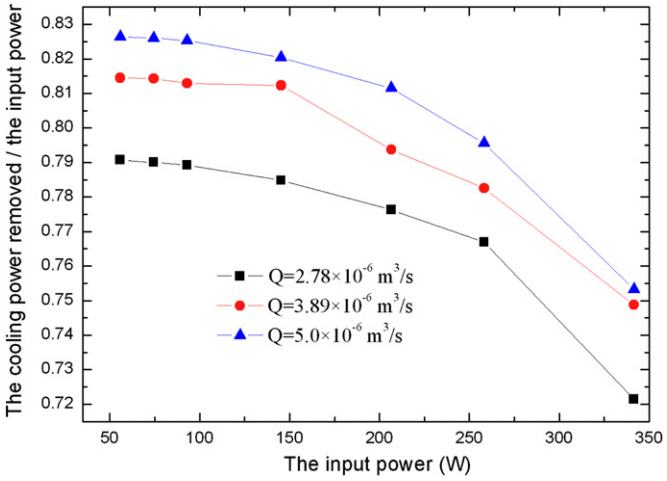


**Fig. 3.** The cooling power removed by the system versus the input power.

### 4.2. Effect of the liquid volume flow rate on the heat transfer

The nozzle-to-surface distance is fixed at $1.451 \times 10^{-2}$ m. The de-ionized water at 298K is sprayed onto the heated surface at various volume flow rates. Fig. 5 shows the heat transfer characteristics in terms of the Weber number. The droplet Weber number is defined as [14]:

$$We = \rho_l u_0^2 d_{32}/\sigma. \tag{5}$$

Here $u_0$ is estimated by the following equation [14]:

$$u_0 = \left(u_j^2 + 2\Delta P/\rho - 12\sigma/(\rho d)\right)^{0.5}. \tag{6}$$

Note that $u_j$ in Eq. (6) is defined as$4Q/\pi d_j^2$. $d$ is obtained from the following equation [14]:

$$d = 9.5 d_j/(\Delta P_1 \sin(\alpha/2)). \tag{7}$$

The Weber number is directly proportional to the liquid volume flow rate from the above derivations.

Fig. 5(a) shows the test surface temperature versus the heater input power in the three cases of different Weber numbers ($We$ = 343, 548 and 609). The Weber number effect is clearly recorded. The surface temperature decreases with the increase of Weber number under the same input power. Increasing the input power enhances the surface temperature significantly. The surface temperature maintains lower than 363 K in the most of test conditions. The design of the present experiment system meets the cooling requirement of high-power solid-state lasers.

The test surface heat flux versus the surface temperature for different Weber numbers ($We$ = 343, 548 and 609) is shown in Fig. 5(b). As seen from the figure, the slope of the curve for $We$ = 609 is the largest; then is the curve for $We$ = 548; and the slope of the curve for $We$ = 343 is the smallest. The heat flux is substantially increased with increasing the Weber number under the same surface temperature. The high Weber number

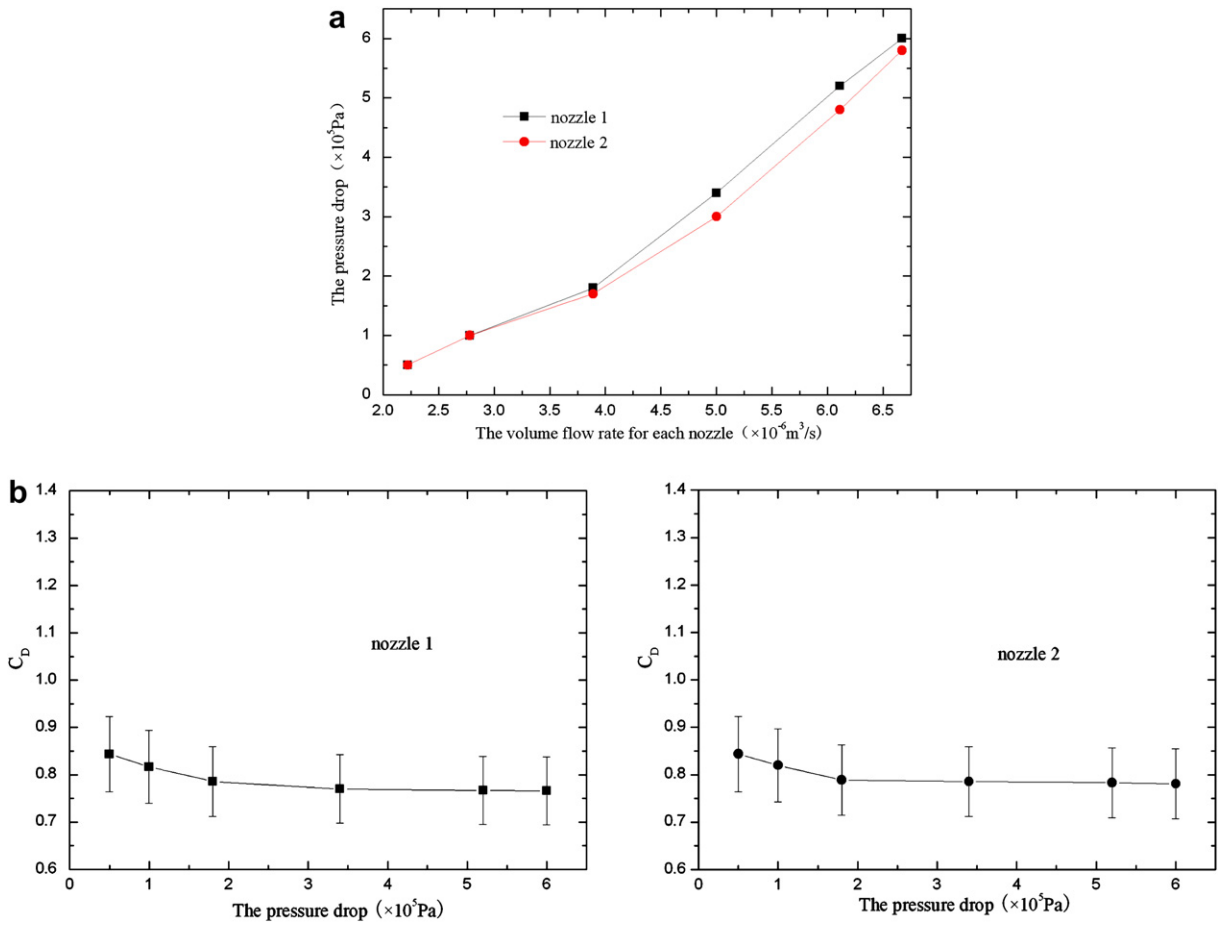


**Fig. 4.** (a) The relation of the volume flow rate versus the pressure drop; (b) the flow coefficients of the nozzles.

characterizes the droplets impacting the liquid film much more strongly and promotes the disturbance between the liquid and the surface. Thus the cooling performance improves. The slop of each curve does not vary much with the surface temperature. Therefore, the heat transfer of the non-boiling spray cooling is mainly ruled by the forced convection along with evaporation from the surface of the liquid film.

Fig. 6 shows the heat transfer coefficients in terms of Reynolds number. The heat transfer coefficient is defined as

$$h = q/(T_w - T_l) \tag{8}$$

It can be seen from Fig. 6 that the heat transfer coefficient increases significantly with increasing *Re*. The cooling performance also improves simultaneously. A coefficient value about $7 \times 10^4$ W/m$^2$K is obtained in the case of $Re = 1900$ and $Q = 6.67 \times 10^{-6}$ m$^3$/s, which is much greater than that occurring in traditional water forced convection or pool boiling heat transfer.

Generally increasing the liquid volume flow rate can improve the spray cooling performance significantly. Because the nozzle inlet pressure increases accompanied with increasing the liquid volume flow rate, the spray energy used to impede the droplets splitting enhances. Both the number of droplets and the total area of the heat transfer become larger. The atomization effect is improved and the heat transfer coefficient is augmented as well. In addition, the droplet collision speed improves with the increase of liquid volume flow rate. Then the corresponding maximum film thickness on the heated surface declines. Due to the heat conduction from the surface to the film, the cooling performance would be better for a thinner liquid film.

Following the work by Jiang et al. [15], the Nusselt number can be correlated as a function of Reynolds number and Prandtl number. The Nusselt number, Reynolds number and Prandtl number are defined based on the equivalent diameter of the heated surface as,

$$Nu = hD/k \tag{9}$$

$$\mathrm{Re} = QD/(A\upsilon) \tag{10}$$

$$\mathrm{Pr} = \upsilon/a \tag{11}$$

Diameter of droplets is probably a better parameter to define Reynolds number and Nusselt number but there can be a significant uncertainty associated with it. Liquid properties are evaluated using mean values of the surface temperature and spray temperature.

A relationship for *Nu* is obtained as,

$$Nu = 0.6751\mathrm{Re}^{0.77}\mathrm{Pr}^{0.84}. \tag{12}$$

The relationship is valid for the Reynolds number in the range of 520–2600 and the Prandtl number in the range of 2.09–7.74.

### 4.3. Effect of the nozzle-to-surface distance on the heat transfer

Fig. 7(a) shows the test surface temperature versus the heater input power in the cases of the nozzle-to-surface distance being $1.151 \times 10^{-2}$, $1.451 \times 10^{-2}$, $1.774 \times 10^{-2}$ and $2.109 \times 10^{-2}$ m, respectively; while the liquid volume flow rate and the inlet

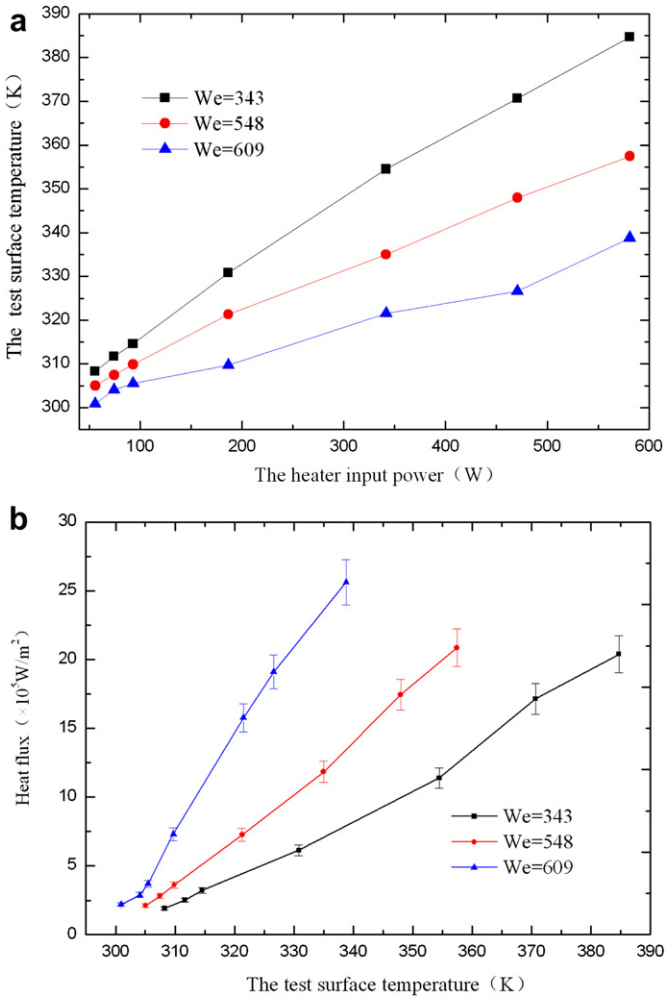


**Fig. 5.** Effect of the liquid volume flow rate on the heat transfer characteristics with regard to the Weber number; (a) the test surface temperature versus the heater input power; and (b) the test surface heat flux versus the surface temperature.

temperature remain unchanged. For each input power, the surface temperature decreases at first and then increases when the distance increases from $1.151 \times 10^{-2}$ to $2.109 \times 10^{-2}$ m. The corresponding heat transfer coefficients change reversely as shown in Fig. 7(b).

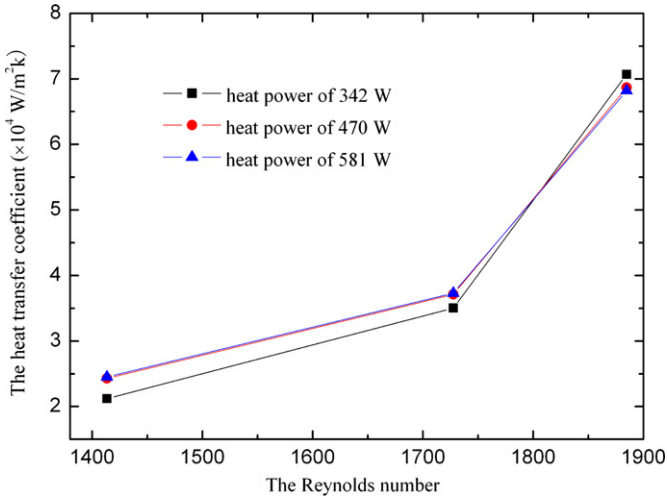


**Fig. 6.** The heat transfer coefficient for different input power values with regard to the Reynolds number.

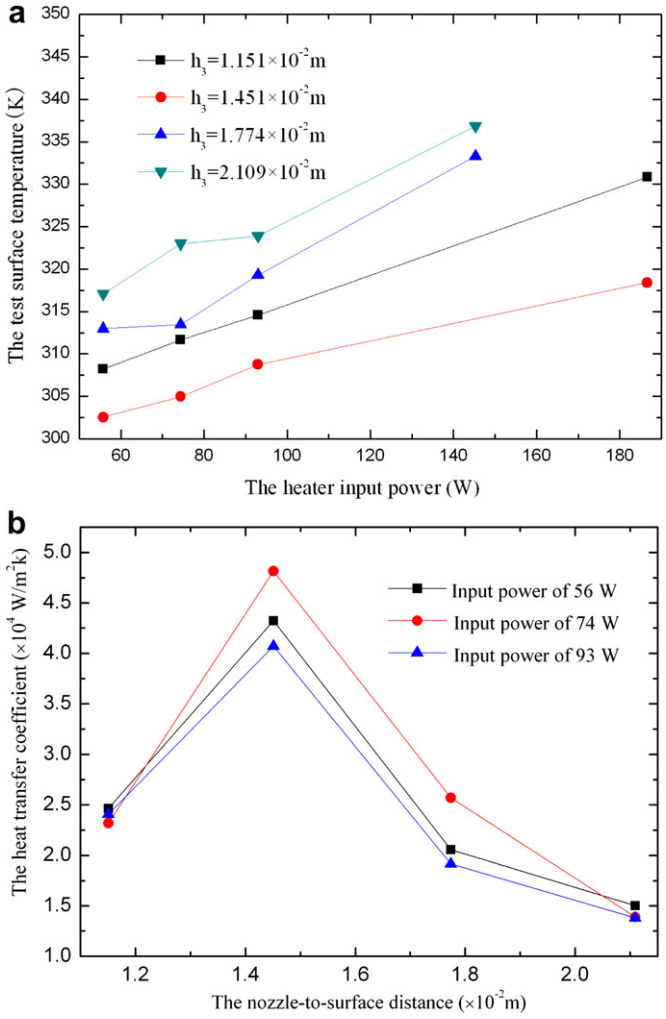


**Fig. 7.** Effect of the nozzle-to-surface distance on the heat transfer; (a) the surface temperature versus heater input power; and (b) the heat transfer coefficient versus the nozzle-to-surface distance.

There exists an optimal distance under which the spray just covers the test surface completely and the heat transfer capability can be maximized. The cooling performance is poor if the distance is too long because some liquid sprays outside the test surface and the effective flow covering the test surface reduces. And if the nozzle-to-surface distance is too short, the surface area wetted will reduce and the cooling performance will also be poor. The optimal distance is $1.451 \times 10^{-2}$ m for the current experimental setup.

### 4.4. Effect of the liquid inlet temperature on the heat transfer

Fig. 8(a) shows the effect of the liquid inlet temperature on the surface temperature in the cases of different input powers. The surface temperature decreases as the liquid inlet temperature reduces. Fig. 8(b) shows the heat transfer coefficient versus the volume flow rate in the two cases of different liquid inlet temperatures. The coefficient in the case of 288.1 K is greater than that in the case of 300.6 K. It is found that the cooling effects will improve significantly with the decrease of the liquid inlet temperature.

### 4.5. Effect of surfactant on the heat transfer

The experiments to determine whether surfactant has any significant effect on the heat transfer are performed by using

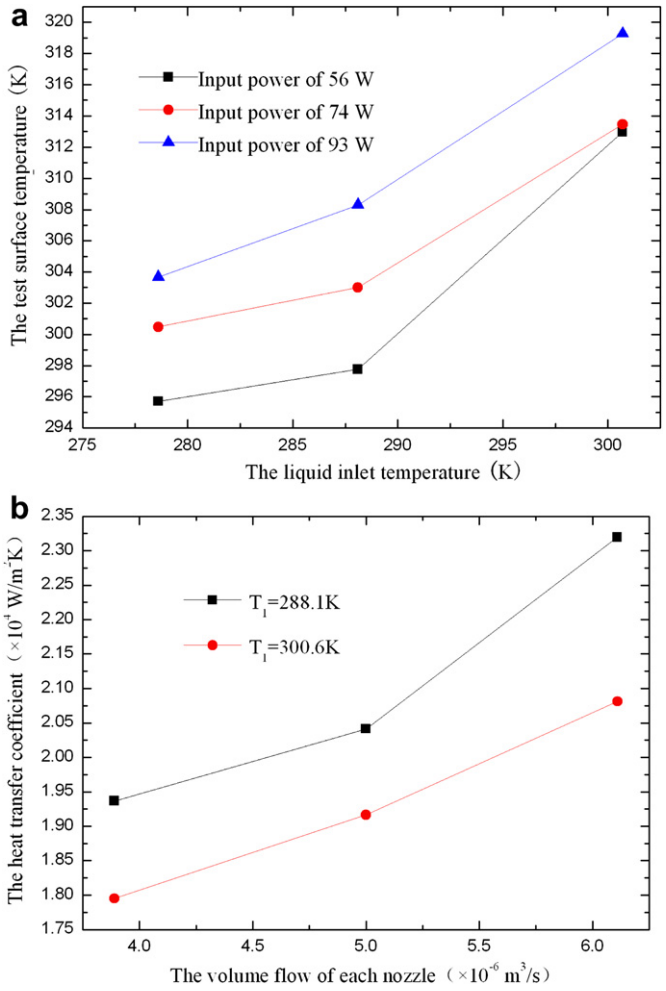


**Fig. 8.** Effect of the liquid inlet temperature on the heat transfer; (a) the surface temperature versus the liquid inlet temperature; and (b) the heat transfer coefficient versus the volume flow rate of each nozzle.

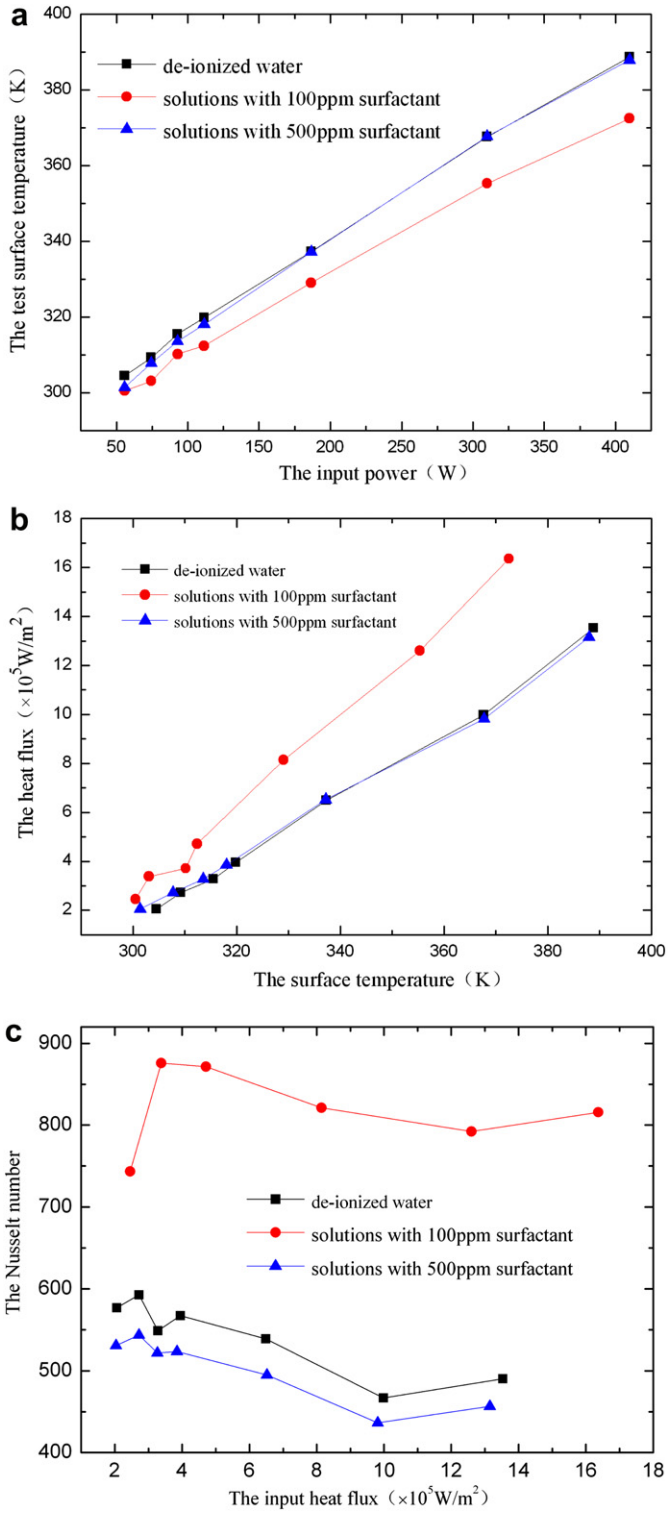


**Fig. 9.** Effect of the surfactant on the heat transfer; (a) the surface temperature versus the input power; (b) the surface heat flux versus the surface temperature; and (c) the Nusselt number versus the input heat flux.

solutions containing 100 ppm and 500 ppm by weight of a surfactant (sodium dodecyl sulfate), respectively. The results are compared with those using the pure de-ionized water. Fig. 9(a) shows the surface temperature variations with the input heater power in the cases of pure de-ionized water, surfactant solutions of 100 ppm and 500 ppm. It is seen that adding 100 ppm surfactant reduces the test surface temperature. However, adding 500 ppm surfactant has no obvious effect on the surface temperature. Fig. 9 (b) shows the surfactant effect on the surface heat flux. Adding 100 ppm surfactant increases the heat flux significantly. In the case of surface temperature being 372 K, the heat flux is increased by 51%. Again, no obvious effect is observed in the case of adding 500 ppm surfactant. Fig. 9(c) shows the effect of the surfactant on the Nusselt number. Adding 100 ppm surfactant increases the Nusselt number by up to 40%. On the contrast, adding 500 ppm surfactant reduces the Nusselt number. It is clear that addition of surfactant may enhance the non-boiling spray cooling heat transfer. The surfactant produces a large change in surface tension of the liquid and improves the atomization conditions. It has been demonstrated that the surfactant reduces the liquid-solid contact angle [16], which is responsible for heat transfer enhancement. The concentration of the surfactant plays an important role on the cooling effect. A very high concentration will weaken the cooling performance due to its poor thermal properties.

## 5. Conclusions

An open-loop non-boiling spray cooling test system using two nozzles in a spray chamber is set up. The heat transfer of non-boiling spray cooling is investigated. The effects of liquid volume

flow rate, liquid inlet temperature, nozzle-to-surface distance and addition of surfactant on the heat transfer are examined. Based on the experimental measurements, the following conclusions can be made:

(1) The technique of non-boiling spray cooling can remove a great deal of heat from surfaces while maintaining the surfaces at low temperature. The heat transfer mechanism consists of both the forced convective heat transfer and the direct evaporation from the surface of the liquid film.
(2) Increasing the liquid volume flow rate or reducing the liquid inlet temperature can improve the spray cooling performance significantly. When increasing the nozzle-to-surface distance, the heat transfer coefficient experiences increase at the beginning and then decrease. Therefore there exists an optimal distance. For this experiment the optimal distance is found to be $1.451 \times 10^{-2}$ m.
(3) The cooling effect can be improved further by adding surfactant with an appropriate concentration. The concentration of surfactant plays an important role in the spray cooling performance.

## Acknowledgements

This research was supported by National Natural Science Foundation of China under Grant No. 50776087 and National Basic Research Program of China under Grant No. 2011CB710705.

## References

[1] L.C. Chow, M.S. Sehembey, M.R. Pais, High heat flux spray cooling, Annu. Rev. Heat Transfer 8 (1997) 291–318.
[2] D.P. Rini, R. Chen, L.C. Chow, Bubble behavior and nucleate boiling heat transfer in saturated FC-72 spray cooling, J. Heat Transfer 124 (2002) 63–72.
[3] C. Bonacina, S.D. Giudice, G. Comini, Dropwise evaporation, J. Heat Transfer 101 (1979) 441–446.
[4] S. Toda, A study of mist cooling (1st report: investigation of mist cooling), Heat Transfer-Jpn. Res. 1 (1972) 54–64.
[5] K.K. Zheng, S.Y. Lei, J.P. Chen, W.J. He, Y. Yao, Effects of liquid flow rate and surface-to-nozzle distance on non-boiling heat transfer performance in spray cooling, Industry Heating 5 (2002) 7–10.
[6] M. Fabbri, S.J. Jiang, V.K. Dhir, A comparative study of cooling of high power density electronics using sprays and microjets, J. Heat Transfer 127 (2005) 38–48.
[7] A.G. Pautsch, T.A. Shedd, Adiabatic and diabatic measurements of the liquid film thickness during spray cooling with FC-72, Int. J. Heat Mass Transfer 49 (15–16) (2006) 2610–2618.
[8] A.G. Pautsch, T.A. Shedd, Spray imipingement cooling with single- and multiple-nozzle arrays. Part I: heat transfer data using FC-72, Int. J. Heat Mass Transfer 48 (2005) 3167–3175.
[9] Z.C. An, S.Y. Lei, W.J. He, J.P. Chen, J.Z. Hao, K.K. Zheng, Electric measurement of the liquid turbulent film under spraying, J. Eng. Thermophys. 25 (1) (2004) 121–123.
[10] C.F. Ma, Y.P. Gan, Y.C. Tian, D.H. Lei, T. Gomi, Liquid jet impingement heat transfer with or without boiling, J. Therm. Sci. 2 (1) (1993) 32–49.
[11] C.H. Amon, J. Murthy, S.C. Yao, S. Narumanchi, C.F. Wu, C.C. Hsieh, MEMS-enabled thermal management of high-heat-flux devices EDIFICE: embedded droplet impingement for integrated cooling of electronics, Exp. Therm. Fluid Sci. 25 (2001) 231–242.
[12] D.N.T. Nguyen, R.H. Chen, L.C. Chow, Effects of heater orientation and confinement on liquid nitrogen pool boiling, J. Thermophys. Heat Transfer 14 (2000) 109–111.
[13] L. Lin, R. Ponnappan, K. Yerkes, B. Hager, Large Area Spray Cooling. Proc. 42nd AIAA Aerospace Sciences Meeting and Exhibit, Reno, NV, 2004.
[14] S.S. Hsieh, T.C. Fan, H.H. Tsai, Spray cooling characteristics of water and R-134a. Part I: nucleate boiling, Int. J. Heat Mass Transfer 47 (2004) 5703–5712.
[15] S.J. Jiang, V.K. Dhir, Spray cooling in a closed system with different fractions of non-condensibles in the environment, Int. J. Heat Mass Transfer 47 (2004) 5391–5406.
[16] C.H. Wang, V.K. Dhir, Effect of surface wettability on active nucleation site density during pool boiling of water on a vertical surface, J. Heat Transfer 115 (1993) 659–669.